

Effect of LOS/NLOS Propagation on Ultra-Dense Networks

Carlo Galietto¹, Nuno K. Pratas², Linda Doyle¹, Nicola Marchetti¹

1) CTVR, Trinity College, Dublin, Ireland

2) Department of Electronic Systems, Aalborg University (AAU), Denmark

1) {galiotc, Linda.Doyle, marchetn}@tcd.ie, 2) nup@es.aau.dk.

Abstract

This paper aims at investigating the achievable performance and the issues that arise in ultra-dense networks (UDNs), when the signal propagation includes both the Line-of-Sight (LOS) and Non-Line-Of-Sight (NLOS) components. Backed by an analytical stochastic geometry-based model, we study the coverage, the Area Spectral Efficiency (ASE) and the energy efficiency of UDNs with LOS/NLOS propagation. We show that when LOS/NLOS propagation components are accounted for, the network suffers from low coverage and the ASE gain is lower than linear at high base station densities. However, this performance drop can partially be attenuated by means of frequency reuse, which is shown to improve the ASE vs coverage trade-off of cell densification, provided that we have a degree of freedom on the density of cells. In addition, from an energy efficiency standpoint, cell densification is shown to be inefficient when both LOS and NLOS components are taken into account. Overall, based on the findings of our work that assumes a more advanced system model compared to the current state-of-the-art, we claim that highly crowded environments of users represent the worst case scenario for ultra-dense networks. Namely, these are likely to face serious issues in terms of limited coverage.

Index Terms

Ultra-dense, LOS/NLOS, Area Spectral Efficiency, partially loaded, energy efficiency, coverage.

I. INTRODUCTION

There is a common and widely shared vision that next generation wireless networks will witness the proliferation of small-cells. As a matter of fact, researchers foresee network densification as one of key enablers of the 5th generation (5G) wireless networks [1], [2]. Although it

refers to a concept rather than being a precise definition, the term *ultra-dense networks* is used to describe networks characterized by a massive and dense deployment of small-cells, in which the amount of base stations may grow up to a point where it will exceed the amount of user devices [3].

As wireless networks evolve, performance requirements for the new technology are becoming more and more stringent. In fact, the 5G requirements are set to a data rate increase up to a 1000-fold with respect to current 4G systems [2], as well as for high energy efficiency [4] in order to limit the energy expenditure of network operators. Supported by recent results [2], [5], cell densification has been put forward as the main enabler to achieve these target data rates. For example, the authors in [5] have shown that the throughput gain is expected to grow linearly with the density of base stations per area; this is a result of the simplified system model used during the investigation. Namely, the assumption of a single slope path-loss model and that all base stations in the network are active.

Nonetheless, further work on cell densification has shown that, under less ideal assumptions, network performance may be different than what predicted in [5]. In particular, when different path-loss models than single slope are used, the actual performance of cell densification is less optimistic than what estimated with single slope path-loss [6]–[9]. In addition, if the base station density increases beyond the user density, like in a typical ultra-dense scenario, the network has been shown to experience a coverage improvement at the expense of a limited throughput gain [3], [10]. This implies that a larger number of BSs will need to be deployed to meet a given data rate target, translating on higher network infrastructures costs.

A. *Related Work*

In recent years, stochastic geometry has been gradually accepted as a mathematical tool for performance assessment of wireless networks. In fact, one of the most important contribution to the study of cell densification can be found in [5], where the authors proposed a stochastic geometry-based framework to model single-tier cellular wireless networks; by assuming a single slope path loss model, the authors have observed the independence of the Signal-to-Interference-plus-Noise-Ratio (SINR) and Spectral Efficiency (SE) from the BS deployment density, with the main consequence being the linear dependence of the ASE on the cell density.

Nevertheless, when the assumption of single-slope path-loss is dropped, it emerges that SINR,

ASE and coverage exhibit a different behaviour than what was found in [5]. The authors in [6], [11] considered propagation models for millimeter waves. In [6], the authors extended the stochastic geometry framework proposed in [5] to a multi-slope path loss model. The authors in [11] developed a stochastic geometry framework for path-loss including Line-of-Sight (LOS) and Non-Line-of-Sight (NLOS) propagation for millimeter-waves. The effect of NLOS propagation on the outage probability has been studied in [7], where the authors propose a function that gives the probability to have LOS at a given point depending on the distance from the source, on the average size of the buildings and on the density of the buildings per area. A stochastic geometry-based framework to study the performance of the network with a combined LOS/NLOS propagation for micro-waves can be found in some previous work of ours [8] and in [9]. The common picture that emerges from the work [6]–[9] is that of a non-linear behavior of the ASE with the cell density; overall, as a consequence of a different propagation model than the single slope path-loss, the spectral efficiency and coverage of the network do actually depend on the base station density. However, all these studies are based on the assumption of fully loaded networks, i.e., all the base stations are active and have at least one user to serve; thus, the applicability of the work above is limited to networks in which the density of base stations is lower than that of the users. In our paper, we broaden the study of network densification to the case where there is no such a constraint in terms of BS density, i.e., we also tackle partially loaded networks, in which some base stations might be inactive.

Work on stochastic geometry for partially loaded networks has been advanced in [3], [10], [12], [13]. The authors in [12] studied the coverage in single tier networks, while multi-tier networks are addressed in [13]. An analysis of the area spectral efficiency of partially loaded networks has been carried out in [3], while in [10] the authors have extended the stochastic geometry-based model further to include multi-antenna transmission, and have also assessed the energy efficiency. Overall, the authors in [10], [12], [13] have shown that the network coverage improves as the base station density increases beyond the user density; this is paid in terms of a lower throughput gain, which grows as a logarithmic function of the cell density. Nonetheless, the authors in [10], [12], [13] modeled the propagation according to a single slope path-loss model and did not investigate the effect of LOS/NLOS propagation in partially loaded networks.

To the best of our knowledge, currently there is no work that addresses ultra-dense scenarios with path-loss models different than the single slope for both fully and partially loaded networks.

As a result of the combined effect of the path-loss model and of the partial load in ultra-dense networks, until now the behavior of the Area Spectral Efficiency (ASE), coverage, and energy efficiency as the networks become denser, was unknown.

B. Our Contribution

This paper seeks to investigate the cell densification process in ultra-dense networks and evaluate the effect of LOS/NLOS propagation on performance metrics such as coverage, spectral efficiency, area spectral efficiency, and energy efficiency. Specifically, we use *ultra-dense networks* as a term to refer to those networks characterized by a very high density of base stations and that include both the cases of *fully loaded networks* (i.e., networks in which all the base stations are active) and *partially loaded networks* (i.e., networks in which some base stations might be inactive and not transmit to any user). Overall, the major contributions of our work can be summarized in the following points:

1) Stochastic geometry-based model for ultra-dense networks with LOS/ NLOS propagation: We propose a model based on stochastic geometry that allows us to study the Signal-to-Interference-plus-Noise-Ratio (SINR) distribution, the spectral efficiency and the area spectral efficiency of ultra-dense networks where the propagation has LOS and NLOS components. We build on previous work [5] and we adapt the model proposed by Andrews et al. to the case of LOS/NLOS propagation. In addition, our framework takes also into account the partial load of ultra-dense networks, in which a fraction of base stations may be inactive.

2) Study of cell densification, partial load and frequency reuse in networks where signal follows LOS/NLOS propagation: First, we investigate the effect of network densification on performance metrics such as SINR, spectral efficiency and area spectral efficiency in networks where the path-loss follows the LOS/NLOS propagation. In particular, the ASE gain becomes lower than linear at high cell densities, meaning that a larger number of BSs would be necessary to achieve a given target with respect to the case of single slope path loss. Moreover, the network coverage drops drastically as the BS density increases. Then, we show that the performance drop due to LOS/NLOS propagation gets mitigated by the usage of frequency reuse or if the base station density exceeds the user density, as it is likely to occur in ultra-dense networks. To the best of our knowledge, the combined effect of LOS/NLOS propagation and partial load/frequency reuse has not been addressed before.

3) Investigation on the minimum transmit power per BS and energy efficiency for networks where signal propagates according to LOS/NLOS path-loss: As the cell density increases, the transmit (TX) power per base station can be lowered. We evaluate the minimum TX power per BS such that the network is guaranteed to be in the interference-limited regime, in which case the performance is not limited by the TX power. Second, we make use of the TX power to determine the energy efficiency of the network when the propagation has LOS and NLOS components. We show that the energy efficiency with LOS/NLOS propagation drops considerably with respect to the case of single slope path-loss, making cell-densification costly for the network from an energetic stand-point. We further extend the study of the energy efficiency to frequency reuse and partial load.

C. Paper Structure

The remainder of this paper is organized as follows. In Section II we describe the system model. We show our formulation for computing the SINR, SE and ASE in Section III and we address the energy efficiency in Section IV. In Section V we present and discuss the results while the conclusions are drawn in Section VI.

II. SYSTEM MODEL

In this paper we consider a network of small-cell base stations deployed according to a homogeneous and isotropic Spatial Poisson Point Process (SPPP), denoted as $\Phi \subset \mathbb{R}^2$, with intensity λ . Further, we assume that each Base Station (BS) transmits with an isotropic antenna and with the same power, P_{TX} , of which the value is not specified, in order to keep our model general and valid for different base station classes (e.g., micro-BSs, pico-BSs, femto-BSs); we focus our analysis on the downlink.

A. Channel model

In our analysis, we considered the following path loss model:

$$\text{PL}(d) = \begin{cases} K_{\text{L}}d^{-\beta_{\text{L}}} & \text{with probability } p_{\text{L}}(d), \\ K_{\text{NL}}d^{-\beta_{\text{NL}}} & \text{with probability } 1 - p_{\text{L}}(d), \end{cases} \quad (1)$$

where β_L and β_{NL} are the path-loss exponents for LOS and NLOS propagation, respectively; K_L and K_{NL} are the signal attenuations at distance $d = 1$ for LOS and NLOS propagation,¹ respectively; $p_L(d)$ is the probability of having LOS as a function of the distance d . The model given in (1) is used by the 3GPP to model the LOS/NLOS propagation, for example, in scenarios with Heterogeneous Networks [14, Table A.2.1.1.2-3]. The incorporation of the NLOS component in the path loss model accounts for possible obstructions of the signal due to large scale objects (e.g. buildings), which will result in a higher attenuation of the NLOS propagation compared to the LOS path. We further assume that the propagation is affected by Rayleigh fading, which is exponentially distributed $\sim \exp(\mu)$.

Regarding the shadow fading, it has been shown that in networks with a deterministic, either regular or irregular, base station distribution affected by log-normal shadow fading, the statistic of the propagation coefficients converges to that of a network with SPPP distribution as the shadowing variance increases [15]. In other words, this SPPP intrinsically models the effect of shadow fading.

B. LOS probability function

To ensure that our formulation and the outcomes of our study are general and not limited to a specific LOS probability pattern, we consider two different LOS probability functions. The first one, which is proposed by the 3GPP [14, Table A.2.1.1.2-3] to assess the network performance in pico-cell scenarios, is given below:

$$p_{L,3G}(d) = 0.5 - \min\left(0.5, 5e^{-\frac{d_0}{d}}\right) + \min\left(0.5, 5e^{-\frac{d}{d_1}}\right), \quad (2)$$

with d_0 and d_1 being two parameters that allow (2) to match the measurement data. Unfortunately, this function is not practical for an analytical formulation. Therefore, we chose to approximate it with a more tractable one, namely:

$$p_L(d) = \exp\left(-\left(\frac{d}{L}\right)^2\right), \quad (3)$$

where L is a parameter that allows (3) to be tuned to match (2). The second function is also suggested by the 3GPP [14, Table A.2.1.1.2-3] and is given below:

$$p_L(d) = \exp(-d/L). \quad (4)$$

¹The parameters K_L and K_{NL} can either refer to the signal attenuations at distance $d = 1$ m or $d = 1$ km; this depends on the actual values given for the parameters of the channel model.

From a physical stand point, the parameter L can be interpreted as the LOS likelihood of a given propagation environment as a function of the distance.

C. User distribution, fully and partially loaded networks

In our model, we always assume that: (i) the users are uniformly distributed; (ii) that each user's position is independent of the other users' position; and (iii) each user connects only to one base station, the one that provides the strongest signal. We denote by λ_U the density of users per area; whenever we consider a finite area A , N_U indicates the average number of users in the network. We also assume the users are served with full buffer, i.e., the base station has always data to transmit to the users and make full use of the available resources.

Depending on the ratio between the density of users and the density of base stations, we distinguish between two cases, namely, fully loaded and partially (or fractionally) loaded networks. By fully loaded networks we refer to the case where each BS has at least one user to serve. With reference to a real scenario, fully loaded networks model the case where there are many more users than base stations, so that each base station serves a non-empty set of users.

However, when the density of users is comparable with or even less that of base stations, some base stations may not have any users to serve and would then be inactive, meaning that they do not transmit and do not generate interference. When this occurs, we say that the network is partially loaded. The network can be modelled as partially loaded to study those scenarios characterized by high density of base stations and, in particular, scenarios where the density of base stations exceeds the density of users, such as in ultra-dense networks.

To define formally the concepts of fully and partially loaded networks, we first need to introduce another concept, which is the *probability a base station being active*.

Definition 1 (Probability of a base station being active). *The probability of a base station being active, denoted as p_A , is the probability that a base station has at least one user to serve. This event implies that the base station is active and transmits to its users.*

Definition 2 (Fully loaded and partially loaded networks). *The network is said to be fully loaded if $p_A = 1$; the network is said to be partially or fractionally loaded if $p_A < 1$.*

III. SINR, SPECTRAL EFFICIENCY AND ASE

In this section we propose an analytical model to compute the SINR Complementary Cumulative Distribution Function (CCDF), which allows us to assess key performance metrics such as coverage, spectral efficiency and ASE.

A. Procedure to compute the SINR CCDF

In order to compute the SINR tail distribution (i.e., the Complementary CDF), we extend the analytical framework first proposed in [5] so that to include the LOS and NLOS components. From the Slivnyak's Theorem [16, Theorem 8.10], we consider the *typical user* as the focus of our analysis, which for convenience is assumed to be located at the origin. The procedure is composed of two steps: (i) we compute the SINR CCDF for the typical user conditioned on the distance from the user to the serving base station, denoted as r ; (ii) using the PDF of the distance from the closest BS $f_r(R)$, which corresponds to the serving BS, we can average the SINR CCDF over all possible values of distance r .

Let us denote the SINR by γ ; formally, the CCDF of γ is computed as:

$$P[\gamma > y] = E_r[P[\gamma > y|r]] = \int_0^{+\infty} P[\gamma > y|r = R] f_r(R) dR. \quad (5)$$

The key elements of this procedure are the PDF of the distance to the nearest base station $f_r(R)$ and the tail probability of the SINR conditioned on r , $P[\gamma > y|r = R]$. The methodology to compute each of these elements while modelling the LOS and NLOS path loss components will be exposed next.

B. SPPPs of base stations in LOS and in NLOS with the user

The set of the base stations locations originates an SPPP, which we denote by $\Phi = \{x_n\}$.² As a result of the propagation model we have adopted in our analysis (see Section II-A), the user can either be in LOS or NLOS with any base station x_n of Φ . Now, we perform the following mapping: we first define the set of LOS points, namely Φ_L , and the set of NLOS points, Φ_{NL} . Then, each point x_n of Φ is mapped into Φ_L if the base station at location x_n is in LOS with the user, while it is mapped to Φ_{NL} if the base station at location x_n is in NLOS with the user. Since the probability that x_n is in LOS with the user is $p_L(\|x\|)$, it follows that each point x_n

²Whenever there is no chance of confusion, we drop the subscript n and use x and instead of x_n for convenience of notation.

of Φ is mapped with probability $p_L(\|x\|)$ into Φ_L and probability $p_{NL}(\|x\|) = 1 - p_L(\|x\|)$ into Φ_{NL} . Given that this mapping is performed independently for each point in Φ , then from the "Thinning Theorem" [16, Theorem 2.36] it follows that the processes Φ_L and Φ_{NL} are SPPPs with density $\lambda_L(x) = \lambda p_L(\|x\|)$ and $\lambda_{NL}(x) = \lambda (1 - p_L(\|x\|))$, respectively. Note that, because of the dependence of $\lambda_L(x)$ and $\lambda_{NL}(x)$ on x , Φ_L and Φ_{NL} are inhomogeneous SPPPs. To make the formulation more tractable, we consider Φ_L and Φ_{NL} to be independent processes; because the union of two SPPPs processes is an SPPP of which the density is the sum of the densities of the individual SPPPs [17, Proposition 1.3.3], the union of Φ_L and Φ_{NL} is an SPPP with density $\lambda_L(x) + \lambda_{NL}(x) = \lambda$, i.e., it is an SPPP with the same density as that of the original process Φ . Hence, the assumption of independence between Φ_L and Φ_{NL} does not alter the nature of the process Φ .

C. Mapping the NLOS SPPP into an equivalent LOS SPPP

Given that we have two inhomogeneous SPPP processes, it is not trivial to obtain the distribution of the minimum distance of the user to the serving base station, which will be necessary later on to compute the SINR CDF. In fact, assuming the user be in LOS with the serving base station at a distance d_1 , there might be an interfering BS at a distance $d_2 < d_1$ which is in NLOS with the user. This is possible because the NLOS propagation is affected by a higher attenuation than the LOS propagation.

Hence, to make our problem more tractable, we map the set of points of the process Φ_{NL} , which corresponds to the NLOS base stations, into an equivalent LOS process Φ_{eq} ; each point $x \in \Phi_{NL}$ located at distance d_{NL} from the user is mapped to a point x_{eq} located at distance d_{eq} from the user, so that the BS located at x_{eq} provides the same signal power to the user with path-loss $K_L d_{eq}^{-\beta_L}$ as if the base station were located at x with path-loss $K_{NL} d_{NL}^{-\beta_{NL}}$.

Definition 3 (Mapping function f_{eq}). *We define the mapping function $f_{eq} : \Phi_{NL} \rightarrow \Phi_{eq}$ as:*

$$f_{eq}(x) = \frac{x}{\|x\|} d_{eq}(\|x\|), \quad (6)$$

$$d_{eq}(d) = \left(\frac{K_L}{K_{NL}} \right)^{1/\beta_L} d^{\beta_{NL}/\beta_L}. \quad (7)$$

Definition 4 (Inverse mapping function g_{eq}). *The inverse function $g_{\text{eq}} = f_{\text{eq}}^{-1} : \Phi_{\text{eq}} \rightarrow \Phi_{\text{NL}}$ is defined as:*

$$g_{\text{eq}}(x) = \frac{x}{\|x\|} d_{\text{eq}}^{-1}(\|x\|), \quad (8)$$

$$d_{\text{eq}}^{-1}(d) = \left(\frac{K_{\text{NL}}}{K_{\text{L}}} \right)^{1/\beta_{\text{NL}}} d^{\beta_{\text{L}}/\beta_{\text{NL}}} = K_{\text{eq}} d^{\beta_{\text{eq}}}, \quad (9)$$

where $K_{\text{eq}} = \left(\frac{K_{\text{NL}}}{K_{\text{L}}} \right)^{1/\beta_{\text{NL}}}$ while $\beta_{\text{eq}} = \beta_{\text{L}}/\beta_{\text{NL}}$.

It is important to notice that, from the "Mapping Theorem" [16, Theorem 2.34], Φ_{eq} is still an SPPP.

D. PDF of the distance from the user to the serving BS

Using the mapping we introduced in Section III-C, we can compute the PDF $f_r(R)$ of the minimum distance r between the user and the serving BS. We first compute the probability $\text{P}[r > R]$; the PDF can be ultimately obtained from the derivative of $\text{P}[r > R]$ as $f_r(R) = \frac{d}{dR}(1 - \text{P}[r > R])$. Let $B(0, l)$ be the ball of radius l centred at the origin $(0, 0)$. Moreover, we use the notation $\Phi(\mathcal{A})$ to refer to number of points $x \in \Phi$ contained in \mathcal{A} [16]. Using the mapping we introduced in Section III-C the probability $\text{P}[r > R]$ can be found as:

$$\begin{aligned} \text{P}[r > R] &= \text{P}[\Phi_{\text{L}}(B(0, R)) = 0 \cap \Phi_{\text{eq}}(B(0, R)) = 0] \\ &\stackrel{(a)}{=} \text{P}[\Phi_{\text{L}}(B(0, R)) = 0 \cap \Phi_{\text{NL}}(B(0, d_{\text{eq}}^{-1}(R))) = 0] \\ &\stackrel{(b)}{=} \text{P}[\Phi_{\text{L}}(B(0, R)) = 0] \cdot \text{P}[\Phi_{\text{NL}}(B(0, d_{\text{eq}}^{-1}(R))) = 0], \end{aligned} \quad (10)$$

where equality (a) comes from the mapping defined in (8) and in (9), while equality (b) comes from the independence of the processes Φ_{L} and Φ_{NL} . By applying the probability function of inhomogeneous SPPP [16, Definition 2.10], we obtain the following,

$$\text{P}[r > R] = \exp\left(-\int_{B(0, R)} \lambda_{\text{L}}(x) dx\right) \exp\left(-\int_{B(0, d_{\text{eq}}^{-1}(R))} \lambda_{\text{NL}}(x) dx\right). \quad (11)$$

From (11), we can obtain $f_r(R)$, first, by integrating and, second, by computing its first derivative in R . The formulation in (11) is general and thus can be applied to several LOS probability functions $p_{\text{L}}(d)$. Below, we provide the expression of the PDF of the distance from the UE to the serving BS for the LOS functions (3) and (4), respectively.

Result 1. If the LOS probability function is as in (3) and if we denote $d_{\text{eq}}^{-1}(R)$ by R_{eq} , the PDF of the distance to the serving BS is:

$$f_r(R) = - \left(e^{\pi\lambda L^2 e^{-\frac{R^2}{L^2}}} \cdot e^{-\pi\lambda L^2 e^{-\frac{R_{\text{eq}}^2}{L^2}}} \cdot e^{-\pi\lambda R_{\text{eq}}^2} \right) \quad (12)$$

$$\left(-2\pi\lambda R e^{-\frac{R^2}{L^2}} \pi\lambda K_{\text{eq}}^2 2\beta_{\text{eq}} R^{2\beta_{\text{eq}}-1} e^{-\frac{-K_{\text{eq}}^2 R^{2\beta_{\text{eq}}}}{L^2}} - \pi\lambda K_{\text{eq}}^2 2\beta_{\text{eq}} R^{2\beta_{\text{eq}}-1} \right).$$

Result 2. If the LOS probability function is as in (4) and if we denote $d_{\text{eq}}^{-1}(R)$ by R_{eq} , the PDF of the distance to the serving BS is:

$$f_r(R) = - \left(e^{2\pi\lambda L^2 e^{-\frac{R}{L}}} \cdot e^{2\pi\lambda L R e^{-\frac{R}{L}}} \cdot e^{-\pi\lambda R_{\text{eq}}^2} \cdot e^{-2\pi\lambda L^2 e^{-\frac{R_{\text{eq}}}{L}}} \cdot e^{-2\pi\lambda L R_{\text{eq}} e^{-\frac{R_{\text{eq}}}{L}}} \right) \quad (13)$$

$$\left(-2\pi\lambda L e^{-\frac{R}{L}} - 2\pi\lambda(L-R)e^{-\frac{R}{L}} - \pi\lambda K_{\text{eq}}^2 2\beta_{\text{eq}} R^{2\beta_{\text{eq}}-1} \right.$$

$$\left. + 2\pi\lambda L K_{\text{eq}} \beta_{\text{eq}} R^{\beta_{\text{eq}}} e^{-\frac{K_{\text{eq}} R^{\beta_{\text{eq}}}}{L}} + 2\pi\lambda L K_{\text{eq}} \beta_{\text{eq}} R^{\beta_{\text{eq}}-1} (K_{\text{eq}} R^{\beta_{\text{eq}}} - L) e^{-\frac{K_{\text{eq}} R^{\beta_{\text{eq}}}}{L}} \right).$$

We refer to the Appendix for the details of the $f_r(R)$ we have given in (12) and in (13).

E. Spatial process of the interfering of the active base stations

In this framework, we include the cases of partially loaded networks and of frequency reuse and we treat them separately. First, we identify the set of BSs that are active, i.e., those having one or more users to serve. As we focus the analysis on the typical user, we can also identify the set of BSs that act as interferers for that user; an active BS (excluding the one serving the user) is seen as an interferer if that BS transmits over the same band used to serve that user. In the following, we denote by Φ_A the set of active BSs, while we denote by Φ_I the set of the interfering BSs.

Let us consider first the case of frequency reuse, in which all the base stations are active, but each of these only uses a portion of the spectrum, in order to reduce the interference. Since all the base stations are supposed to be active, the process Φ_A is the same as Φ . However, we assume each base station selects a channel in a random manner using, for instance, frequency ALOHA spectrum access [18]. With a frequency reuse factor of N , each base station uses 1 out of N channels, which is chosen independently from the other base stations. Hence, each BS interferes with a given user with probability $1/N$; this is equivalent to carrying out a thinning

of the original process Φ with probability $1/N$; from the Thinning Theorem, we obtain that Φ_I is a homogeneous process with density $\lambda_I = \lambda/N$.

In regards to the partially loaded networks, we recall from Section II-C that a fraction of the base stations might be inactive and, as such, would not generate interference. Assuming all the BSs transmit over the same band, in partially loaded networks the active base stations are the only BSs that generate interference to the users—with the exception of the serving BS. Thus, we can write $\Phi_I = \Phi_A \setminus x_0$, where x_0 is the serving base station; moreover, from the Palm Theorem [16], Φ_I and Φ_A are characterized by the same density. To obtain the process of active BSs Φ_A from the original the process Φ , we first assume that each UE deployed in the network connects to the closest BS;³ finally, only the BSs which are assigned one or more users are active. Yet, this is equivalent to performing a thinning of the original process to obtain Φ_A . However, the fact that a base station is picked to be part of Φ_A (i.e. there exists a user for which this BS is the closest one) depends on the positions of the neighbouring base stations, which implies that the base stations are not chosen independently of one another [12]. As the independence is one of the necessary conditions in order to have an SPPP, it follows that Φ_A is not an SPPP.

Although Φ_A cannot be formally regarded as an SPPP, it has been shown that the actual SPPP obtained through the thinning of Φ well approximates Φ_A [10], [12]. Specifically, the authors in [12] have shown that, (i) the probability p_A of a base station to be active (i.e., to have users to serve) can be well approximated once the density of users λ_U and density of base stations λ are known, and, (ii) the process Φ_A of active base stations can be well approximated by thinning the original process Φ_A with probability p_A , which is given below [12]:

$$p_A = 1 - \left(1 + \frac{\lambda_U}{3.5\lambda}\right)^{-3.5}. \quad (14)$$

From the Thinning Theorem, it follows that the resulting process obtained through thinning as described above is an SPPP with density $\lambda_A = p_A\lambda$; moreover, $\lambda_I = \lambda_A$. In light of these findings, we approximate Φ_A with an SPPP of density $\lambda_A = p_A\lambda$.

Fig. 1 shows how the probability p_A and the intensity of the interfering BSs λ_I vary as functions of the ratio λ/λ_U .

³As we recall from Section III-C, with LOS/NLOS propagation the serving BS might not be the closest one to the user. Nonetheless, this does not alter the validity of the explanation we are giving in this section.

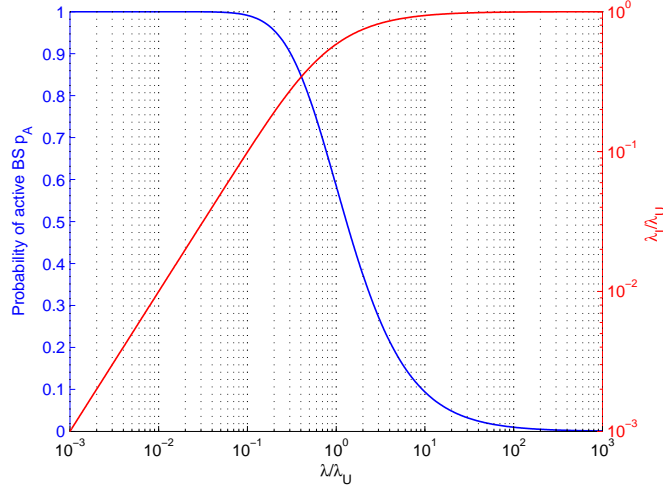


Fig. 1. Probability of a BS being active and density of interfering BS vs BS density for partially loaded networks. The probability p_A drops as the ratio λ/λ_U is close to or greater than 1, i.e., as λ approaches λ_U . As a result of this, the density of active BSs as well as the density of interfering BSs converge to λ_U as λ approaches or overcomes λ_U .

F. SINR inverse cumulative distribution function

The probability $P[\gamma > y | r = R]$ can be computed as in [5, Theorem 1]; we skip the details and provide the general formulation:

$$P[\gamma > y | r = R] = P\left[\frac{gK_L R^{-\beta_L}}{\sigma^2 + I_R} > y\right] = e^{-\mu y K_L^{-1} R^{\beta_L} \sigma^2} \mathcal{L}_{I_R}(\mu y K_L^{-1} R^{\beta_L}), \quad (15)$$

where g is the Rayleigh fading, which we assume to be an exponential random variable $\sim \exp(\mu)$; σ^2 is the variance of the additive white Gaussian noise normalized with the respect to the transmit power, I_R is the interference conditioned on R , i.e.,

$$I_R = \sum_{\{i: x_i \in \Phi_L \cap \Phi_A, \|x_i\| > R\}} g_i K_L \|x_i\|^{-\beta_L} + \sum_{\{j: f_{\text{eq}}(x_j) \in \Phi_{\text{NL}} \cap \Phi_A, \|f_{\text{eq}}(x_j)\| > R\}} g_j K_L \|x_j\|^{-\beta_L} \quad (16)$$

$$= \sum_{\{i: x_i \in \Phi_L \cap \Phi_A, \|x_i\| > R\}} g_i K_L \|x_i\|^{-\beta_L} + \sum_{\{j: x_j \in \Phi_{\text{NL}} \cap \Phi_A, \|x_j\| > d_{\text{eq}}^{-1}(R)\}} g_j K_{\text{NL}} \|x_j\|^{-\beta_{\text{NL}}} \quad (17)$$

where g_i and g_j are independent and identically distributed $\sim \exp(\mu)$ fading coefficients. Please, note that the overall interference accounts only for the active base stations. Compared to the formulation of $\mathcal{L}_{I_R}(s)$ proposed in [5], in our case we have to deal with two non-homogeneous SPPP, namely Φ_L and Φ_{NL} instead of a single homogeneous SPPP. The Laplace transform $\mathcal{L}_{I_R}(s)$

can be written as follows:

$$\mathcal{L}_{I_R}(s) = \mathbb{E}_{\Phi_L \cap \Phi_A, \Phi_{NL} \cap \Phi_A, g_i, g_j} \left[\exp \left(-s \sum_{\{i: x_i \in \Phi_L \cap \Phi_A, |x_i| > |x_0|\}} g_i K_L \|x_i\|^{-\beta_L} \right) \exp \left(-s \sum_{\{j: x_j \in \Phi_{NL} \cap \Phi_A, \|x_j\| > d_{eq}^{-1}(R)\}} g_j K_{NL} \|x_j\|^{-\beta_{NL}} \right) \right].$$

Given that Φ_L and Φ_{NL} are two independent SPPP, we can separate the expectation to obtain:

$$\mathcal{L}_{I_R}(s) = \mathbb{E}_{\Phi_L \cap \Phi_A, g_i} \left[\exp \left(-s \sum_{\{i: x_i \in \Phi_L \cap \Phi_A, \|x_i\| > R\}} g_i K_L \|x_i\|^{-\beta_L} \right) \right] \mathbb{E}_{\Phi_{NL} \cap \Phi_A, g_j} \left[\exp \left(-s \sum_{\{j: x_j \in \Phi_{NL} \cap \Phi_A, \|x_j\| > d_{eq}^{-1}(R)\}} g_j K_{NL} \|x_j\|^{-\beta_{NL}} \right) \right]. \quad (18)$$

By applying the Probability Generating Functional (PGFL) for SPPP (which holds also in case of inhomogeneous SPPP [16]) to (18), we obtain the following result:

Result 3. *The Laplace transform $\mathcal{L}_{I_R}(s)$ for LOS/NLOS propagation with model given in (1) is:*

$$\mathcal{L}_{I_R}(s) = \exp \left(-2\pi\lambda_I \int_R^{+\infty} \left[\frac{sK_L v^{-\beta_L}}{sK_L v^{-\beta_L} + \mu} \right] p_L(v) v dv \right) \exp \left(-2\pi\lambda_I \int_{d_{eq}^{-1}(R)}^{+\infty} \left[\frac{sK_{NL} v^{-\beta_{NL}}}{sK_{NL} v^{-\beta_{NL}} + \mu} \right] p_{NL}(v) v dv \right). \quad (19)$$

The Laplace transform in (19) along with (11) and (A.4) can be plugged in (5) to obtain the SINR CCDF through numerical integration.

G. Average Spectral Efficiency and Area Spectral Efficiency

Similarly to [5, Section IV] we compute the average spectral efficiency and the ASE of the network. First, we define the ASE as:

$$\eta_A = \frac{\lambda_A \cdot A \cdot BW_U \cdot E[C]}{A \cdot BW_A} = \frac{\lambda_A \cdot E[C]}{N}, \quad (20)$$

where BW_A is the available bandwidth, BW_U is the used bandwidth, $E[C]$ is the average spectral efficiency, A is the area, $N_{BS,A}$ is the number of active base stations within the area A , and N

is frequency reuse factor. The average rate $E[C]$ can be computed as follows [5]:

$$E[C] = E[\log_2(1 + \gamma)] = \int_0^{+\infty} P[\log_2(1 + \gamma) > u] du \quad (21)$$

$$\begin{aligned} &= \int_0^{+\infty} \int_0^{+\infty} P[\log_2(1 + \gamma) > u | r = R] f_r(R) dR du. \\ &= \int_0^{+\infty} \int_0^{+\infty} e^{-\mu(2^u - 1)K_L^{-1}R^{\beta_L}\sigma^2} \mathcal{L}_{I_R}(\mu(2^u - 1)K_L^{-1}R^{\beta_L}) f_r(R) dR du \end{aligned} \quad (22)$$

where $\mathcal{L}_{I_R}(s)$ is given in (19). Similarly to the SINR CCDF, (22) can be evaluated numerically.

IV. ENERGY EFFICIENCY WITH LOS/NLOS PROPAGATION

A. Computing the transmit power per base station

We evaluate the TX power in order to compute the overall power consumption of the wireless network. Ideally, to ensure the network performance not be limited by the transmit power, P_{TX} should be set in order to guarantee the interference-limited regime, i.e., the transmit power should be high enough so that the thermal noise power at the user receiver can be neglected with respect to the interference power at the receiver. In fact, when the network is in the interference-limited regime, the transmit power is high enough that any further increase of it would be pointless in terms of enhancing the SINR, since the receive power increment would be balanced by the exact same interference increment.

Practically, we refer to the outage probability $\theta = P[\gamma \leq \gamma_{th}]$ as a constraint to set the power necessary to reach the interference limited regime. When the TX power is low, small increments of P_{TX} yields large improvements of the outage θ ; however, as P_{TX} increases, the corresponding outage gain reduces, until θ eventually converges to its optimal value θ^* , which would be reached in absence of thermal noise. It is reasonable to assume the network be in the interference-limited regime when the following condition is met:

$$|\theta^* - \theta| \leq \Delta_\theta, \quad (23)$$

where Δ_θ is a tolerance measure setting the constraint in terms of the maximum deviation of θ from the optimal value θ^* . Eq. (23) provides us with a metric to compute the transmit power, but does not give us any indication on how to find P_{TX} as a function of the density λ . Unfortunately, we cannot derive a closed-form expression for the transmit power that satisfies (23), as we do

not have any closed-form solution for the outage probability $\theta = P[\gamma \leq \gamma_{\text{th}}]$. We then take a different approach to calculate the minimum transmit power.

In Alg. 1 we proposed a simple iterative algorithm that finds the minimum transmit power satisfying (23) by using numerical integration of (5). This algorithm computes the outage probability corresponding to a given P_{TX} ; starting from a low value of power, it gradually increases P_{TX} by a given power step Δ_P , until (23) is satisfied. To speed up this procedure, the step granularity is adjusted from a coarse step p_1 up to the finest step p_{N_p} , which represents the precision of the power value returned by Alg. 1.

Algorithm 1 Steps to compute the transmit power.

INPUTS:

- 1) Vector of the power steps in dBm $\mathbf{p} = [p_1, \dots, p_{N_p}]$, N_p is the length of vector \mathbf{p} ;
- 2) Outage SINR threshold γ_{th} ;
- 3) Outage tolerance Δ_θ ;

Initialize variables:

- 1) $P_{\text{curr}} = P_{N_0}$, where P_{N_0} is the AWGN power in dBm over the bandwidth BW_U
- 2) $P_{\text{fin}} = P_{\text{curr}}$

Find optimal outage $\theta^* = P[\gamma \leq \gamma_{\text{th}}]$ by integrating (5) with parameter $\sigma^2 = 0$

for $k = 1, \dots, N_p$ **do**

Find $\theta(P_{\text{curr}}) = P[\gamma \leq \gamma_{\text{th}}]$ by integrating (5) with parameter $\sigma^2 = 10^{-\frac{P_{\text{curr}}}{10}}$

Set granularity of the power step $\Delta_P = p_k$

while $|\theta^* - \theta(P_{\text{curr}})| > \Delta_\theta$ **do**

Increase the current power with step Δ_P , i.e., $P_{\text{curr}} = P_{\text{curr}} + \Delta_P$

Find $\theta(P_{\text{curr}}) = P[\gamma \leq \gamma_{\text{th}}]$ by integrating (5) with parameter $\sigma^2 = 10^{-\frac{P_{\text{curr}}}{10}}$

Update the final value of power, i.e., $P_{\text{fin}} = P_{\text{curr}}$

Remove the last power increment before increasing the granularity, i.e., $P_{\text{curr}} = P_{\text{curr}} - \Delta_P$

OUTPUT: P_{fin} is the power in dBm s.t. (23) is satisfied.

B. Energy efficiency

In this subsection, we characterize the energy efficiency of the network as a function of the base station density to identify the trade-off between the area spectral efficiency and the power consumed by network. We define the *energy efficiency* as the ratio between the overall throughput

delivered by the network and the total power consumed by the wireless network, i.e., we define the energy efficiency as follows:

$$\eta_{\text{EE}}(\lambda) \triangleq \frac{T(\lambda)}{P_{\text{TOT}}(\lambda)}, \quad (24)$$

where $T(\lambda)$ is the network throughput, which can be written as $T(\lambda) = A \cdot \text{BW} \cdot \eta_{\text{A}}(\lambda)$, with BW denoting the bandwidth and $\eta_{\text{A}}(\lambda)$ denoting the area spectral efficiency; P_{TOT} is the overall power consumption of the network.

When we compute the power consumption of each BS, we need to take into account that a fraction of the base stations may be inactive and model the power consumption accordingly. For active base station, we model the power consumption $P_{\text{BS,A}}$ of the base station assuming that $P_{\text{BS,A}}$ is the sum of two components, i.e., $P_{\text{BS,A}} = P_0 + P_{\text{RF}}$; the first, denoted by P_0 , takes into account the energy necessary for signal processing and to power up the base station circuitry. This power P_0 is modelled as a component being independent of the transmit power and of the base station load [19]. The second component, denoted by P_{RF} , takes into account the power fed into the power amplifier which is then radiated for signal transmission. The power P_{RF} is considered to be proportional to the power transmitted by the base station; we can thus write $P_{\text{RF}} = K_{\text{RF}}P_{\text{TX}}$, where K_{RF} takes into account the losses of the power amplifier (i.e., we assume K_{RF} to be the inverse of the power amplifier efficiency).

In the case of inactive base stations, we assume that the BS switches to a stand-by state for energy saving purposes [20], in which it does not transmit (i.e., $P_{\text{RF}} = 0$) and reduces the circuitry power consumption. Therefore, the power required to maintain the stand-by state can be modelled as $P_{\text{BS,S}} = \rho P_0$, where ρ is power saving factor that describes the relative power consumption of the circuitry with respect to the active case; note that $0 < \rho < 1$.

Finally, the overall power consumption of the network due to both active and inactive base station can be expressed as follows:

$$\begin{aligned} P_{\text{TOT}} &= A\lambda_{\text{A}}P_{\text{BS,A}} + A(\lambda - \lambda_{\text{A}})P_{\text{BS,S}} \\ &= A\lambda_{\text{A}}P_0 + A\lambda_{\text{A}}P_{\text{TX}}K_{\text{RF}} + A(\lambda - \lambda_{\text{A}})\rho P_0. \end{aligned} \quad (25)$$

The energy efficiency for the cases of fully loaded networks and partially loaded networks is addressed in the following sub-sections.

C. Energy efficiency for fully loaded networks

In this section we study the energy efficiency $\eta_{\text{EE}}(\lambda)$ trend as a function of λ ; we focus on fully loaded networks, i.e., $p_A = 1$ and $\lambda_A = \lambda$. Unfortunately, the analysis of the derivative of η_{EE} is not straightforward, as we have a closed-form solution neither for the throughput $T(\lambda)$ nor for the transmit power $P_{\text{TX}}(\lambda)$. One feasible way to get around this burden is to approximate $T(\lambda)$ and $P_{\text{TX}}(\lambda)$ with functions in the form:

$$f(z) = az^b. \quad (26)$$

The model in (26) has two advantages: (i) it can be easily derivated and, thus, is apt to investigate the existence of optima; (ii) it is well suited to fit the non-linear behaviour of ASE and TX power. In fact, we have shown in our previous work [21] that both $T(\lambda)$ and $P_{\text{TX}}(\lambda)$ can be approximated with a piece-wise function in the form (26), where the parameters a and b can be obtained, for instance, by linear regression in the logarithmic domain for a given range of values of λ .

Backed by the conclusions from previous work [21], we approximate the throughput as $T(\lambda) = AT_0\lambda^\alpha$ and the transmit power as $P_{\text{TX}}(\lambda) = P_T\lambda^\delta$, within a given interval of λ . Under these assumptions, the energy efficiency becomes:

$$\eta_{\text{EE}}(\lambda) = \frac{T_0\lambda^\alpha}{\lambda P_0 + \lambda K_{\text{RF}} P_T \lambda^\delta} = \frac{T_0\lambda^{\alpha-1}}{P_0 + K_{\text{RF}} P_T \lambda^\delta}. \quad (27)$$

The derivative of $\eta_{\text{EE}}(\lambda)$ is given below:

$$\frac{d\eta_{\text{EE}}(\lambda)}{d\lambda} = \frac{T_0 P_0 (\alpha - 1) \lambda^{\alpha-2} + T_0 K_{\text{RF}} P_T (\alpha - \delta - 1) \lambda^{\alpha+\delta-2}}{(P_0 + K_{\text{RF}} P_T \lambda^\delta)^2}. \quad (28)$$

Let us note that T_0 , P_0 , K_{RF} and P_T are positive; moreover it is reasonable to assume that $\alpha > 0$ (i.e., the area spectral efficiency is an increasing function of the density) and that $\delta < 0$, i.e., the transmit power per BS is a decreasing function of the density. In the following paragraphs, we study the behaviour of the energy efficiency as function of the density λ by analyzing the derivative $\eta'_{\text{EE}}(\lambda)$. We distinguish the following three cases.

1) *The energy efficiency is a monotonically increasing function:* This occurs if the ASE growth is linear or superlinear, i.e., if $\alpha \geq 1$. From this, it follows that also $\alpha \geq 1 > 1 + \delta$ holds true; in this case, $\eta'_{\text{EE}}(\lambda)$ is strictly positive, meaning that the energy efficiency increases as the density increases.

2) *The energy efficiency is a monotonically decreasing function:* This occurs if the ASE growth is sublinear, i.e., if $\alpha < 1$, and, in addition, $\alpha < 1 + \delta$. Then, $\eta'_{\text{EE}}(\lambda)$ is strictly negative and so the energy efficiency is a monotonically decreasing function of the density λ .

3) *The energy efficiency exhibits an optimum point:* If ASE gain is sublinear (i.e. $\alpha < 1$) but grows with a slope α sufficiently high, (i.e., $\alpha > 1 + \delta$), then we obtain that the derivative $\eta'_{\text{EE}}(\lambda)$ nulls for

$$\lambda_0 = \left(\frac{P_0(1-\alpha)}{K_{\text{RF}}P_{\text{T}}(\alpha-\delta-1)} \right)^{1/\delta}, \quad (29)$$

is positive for $\lambda < \lambda_0$ and is negative for $\lambda > \lambda_0$. Therefore, λ_0 is a global maximum of the energy efficiency.

As a whole, the behavior of the spectral efficiency is due to how the growths of the ASE of the TX power relate among each other as the base station density increases. If the ASE grows rapidly enough to counterbalance the total power increase of the network given by the addition of base stations, then the energy efficiency increases with the BS density; this means that adding base station is profitable in terms of energy efficiency. Else, adding BSs turns not to be profitable from energy efficiency point of view.

D. Energy efficiency for partially loaded networks

For partially loaded networks, we only analyze the case where $\lambda > \lambda_{\text{U}}$, as the opposite case of $\lambda < \lambda_{\text{U}}$ leads back to fully loaded networks. By using L'Hôpital's rule, one can show that (14) can be approximated by $p_{\text{A}} \cong \lambda_{\text{U}}\lambda^{-1}$, for λ is sufficiently greater than λ_{U} . By applying this approximation to (25), we obtain:

$$P_{\text{TOT}} = \lambda_{\text{U}}P_0(1-\rho) + \lambda\rho P_0 + \lambda_{\text{U}}K_{\text{RF}}P_{\text{T}}\lambda^{\delta}. \quad (30)$$

It is known from [19] that, as the BS density increases, the main contribution to the total power consumption is due to the circuitry power P_0 , while the transmit power becomes negligible for the overall power balance. Therefore, to make the problem more tractable, we can further approximate the total power in (30) as $P_{\text{TOT}} \cong \lambda_{\text{U}}P_0(1-\rho) + \lambda\rho P_0$. From (24), by using the approximation $T(\lambda) = AT_0\lambda^{\alpha}$ for the throughput and $P_{\text{TOT}} \cong \lambda_{\text{U}}P_0(1-\rho) + \lambda\rho P_0$ for the power, we obtain the following expression for the energy efficiency:

$$\eta_{\text{EE}}(\lambda) \cong \frac{T_0\lambda^{\alpha-1}}{\lambda_{\text{U}}P_0(1-\rho) + \lambda\rho P_0}. \quad (31)$$

To analyze the behaviour of the energy efficiency as a function of λ , we follow the same approach as in Section IV-C and we compute the derivative of $\eta_{EE}(\lambda)$, which is given below:

$$\frac{d\eta_{EE}(\lambda)}{d\lambda} = \frac{T_0\lambda^{\alpha-1}(\lambda\rho(\alpha-1) + \alpha\lambda_U(1-\rho))}{(\lambda_U P_0(1-\rho) + \lambda\rho P_0)^2}. \quad (32)$$

As the ASE is known to be sub-linear for partially loaded networks [3], [10], we assume $0 < \alpha < 1$; moreover, the power saving factor ρ satisfies $0 < \rho < 1$. Therefore, the derivative η'_{EE} nulls for:

$$\lambda^* = \frac{\alpha\lambda_U(1-\rho)}{\rho(1-\alpha)}, \quad (33)$$

it is positive for $\lambda < \lambda^*$ while it is negative for $\lambda > \lambda^*$. Hence, λ^* is a local maximum of the energy efficiency for partially loaded networks and the energy efficiency decreases for densities $\lambda > \lambda^*$. Note that, this result holds for λ sufficiently greater than λ_U .

V. RESULTS

In this section we present and discuss the results we obtained by integrating numerically the expressions of outage probability, of the Spectral Efficiency (SE), and of the ASE. In Section V-A, V-B and V-C we assume the network to be interference-limited (i.e., we set the thermal noise power to 0), while the noise is taken into account in Section V-D and V-E.

The parameters we used to obtain our results are specified in Table I.

TABLE I
PARAMETERS FOR RESULTS SECTION

Parameter	Value
Path-loss - Single slope	$PL_{SL}(d_{km}) = 140.7 + 36.7 \log(d_{km})$, $\beta = 3.67$, $K_{SL} = 10^{14.07}$ [14]
Path-loss - Combined LOS/NLOS	See (1); with d in km, $K_L = 10^{10.38}$, $\beta_L = 2.09$, $K_{NL} = 10^{14.54}$, $\beta_{NL} = 3.75$, $d_0 = 0.156\text{km}$, $d_1 = 0.03\text{km}$ [14]
Parameter L	82.5m, set so that (2) and (3) intersect at the point corresponding to probability 0.5
Bandwidth BW	10 MHz centered at 2 GHz
Noise	Additive White Gaussian Noise (AWGN) with -174 dBm/Hz Power Spectral Density
Noise Figure	9 dB
Antenna at BS and UE	Omni-directional with 0 dBi gain
K_{RF}	10 [19]
P_0	10W [19]

A. Spectral efficiency, outage probability and ASE

In this subsection we assume the network to be fully loaded and with frequency reuse 1. We compared the results for two LOS probability functions, namely (3) and (4); we also compared the results for LOS/NLOS propagation with those obtained with a the single slope path-loss model. We first analyze the outage probability (defined as $\theta = P[\gamma \leq \gamma_{\text{th}}]$) results, which have been obtained by numerical integration of (5).

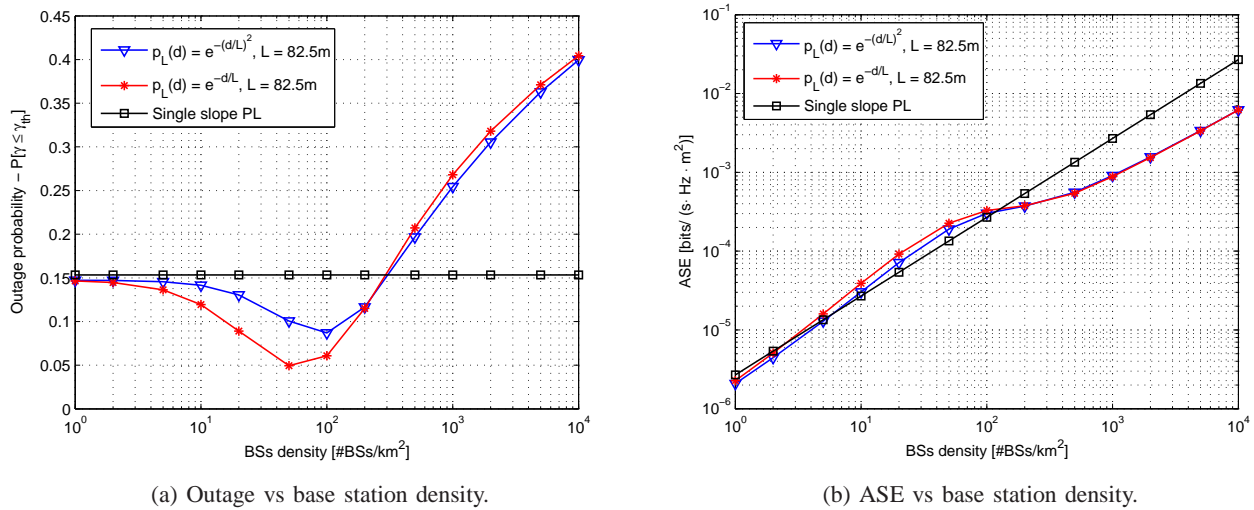


Fig. 2. (a) Outage probability and (b) ASE vs base station density for different LOS probability function.

We show the outage probability results in Fig. 2a, where we can see the different effect of the LOS/NLOS propagation with respect to the single slope Path-Loss (PL). With single-slope PL, the outage is constant with the BS density. In contrast, with LOS/NLOS propagation, there is a minimum in the outage curves, which is achieved for density $\lambda = 50\text{-}100\text{BSs/km}^2$, depending on the LOS probability function. Within this range of densities, the user is likely to be in LOS with the serving BS and in NLOS with most of the interfering BS, meaning that the interference power is lower than the received power.

At densities λ greater than 300BSs/km^2 , the outage starts growing drastically and, depending on the LOS likelihood, can reach 32-43%. This is due to the fact that more and more interfering BSs are likely to enter the LOS region, causing an overall interference growth and thus a reduction of the SIR. At densities λ smaller than 100BSs/km^2 , the serving BS as well as the interfering BSs are likely to be in NLOS with the user. Because of this, both the receive power and the

overall interference increase at the same pace⁴ and, as a consequence, the SIR remains constant, and so does the outage. Let us note that, the LOS probability function affects the outage curves at intermediate values of the BS density (e.g. 10-300 BSs/km²). At low densities, all the BSs are likely to be in NLOS with the user, while at high densities the serving BS and the strongest interferers are likely to be in LOS BSs are likely to be in LOS with the user.

The results of the ASE are shown in Fig. 2b. Compared to the single-slope PL, which shows a linear growth of the ASE with the density λ , with the LOS/NLOS propagation we observe a different behaviour of the ASE. In particular, we observe a lower steepness of the ASE curve at high BS densities, which is due to the effect of the interfering BSs entering the LOS region and, thus, increasing the total interference power.

To assess steepness of the ASE, we can use linear regression to interpolate the ASE curve with the model given in (26). In particular, we can approximate the ASE $\eta_A(\lambda)$ with a piece-wise function of the kind $\eta_A(\lambda) = \eta_{A,0}\lambda^\alpha$, where $\eta_{A,0}$ and α are given for given intervals of λ . We specifically focus on α , which gives the steepness of the ASE curve. With reference to the ASE curve (solid-blue curve in Fig. 2b) obtained with (3) as a LOS probability function, the the value of the parameter α turns to be 1.15 within the range of λ 1-50 BSs/km², 0.48 within the range 50-500 BSs/km² and 0.81 within the range 500-10000 BSs/km².

B. Frequency reuse

To have a comprehensive view of the frequency reuse as an interference mitigation scheme, we need to assess the trade-off between the ASE and the network coverage probability, defined as $1 - P[\gamma \leq \gamma_{th}]$. The results of this trade-off are shown in Fig. 3, where we plotted the network coverage against the ASE for different frequency reuse factors and base station densities.

Firstly, we focus on the LOS/NLOS propagation; we can notice from this plot that, if we fix the BS density, higher frequency reuse factors enhance the network coverage but, on the other hand, determine a drop of the ASE. This is in line with what one would expect from frequency reuse. Nonetheless, if we have no constraint in the choice of the BS density, the ASE vs coverage trade-off improves as the frequency reuse factor increases. In fact, the trade-off curve we obtain

⁴If both serving BS and interfering BS are in NLOS with the user, the path-loss exponents of the serving BS-to-user channel and of the interfering BS-to-user channels are the same and, therefore, the power or the interference and of the received signal varies at the same slope as a function of the density.

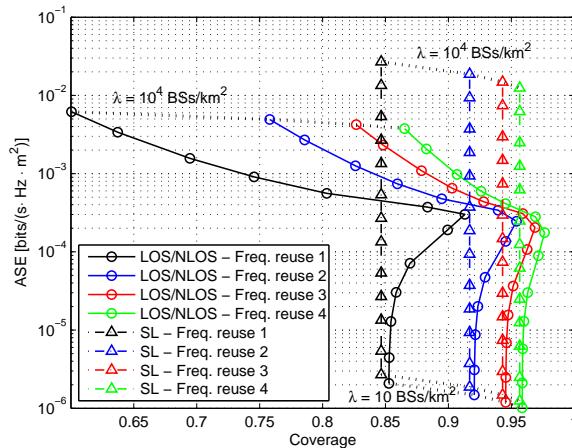


Fig. 3. ASE vs coverage trade-off for frequency reuse. The trade-off curves have been plotted for BS density equal to 10, 20, 50, 100, 200, 500, 1000, 2000, 5000, 10000 BSs/km², and compare the combined LOS/NLOS model with the single slope one.

for a given reuse factor K lies on the top-right hand side with respect to the curve for reuse factor $K - 1$. This means that, by increasing the reuse factor and the base station density at the same time, it is possible to achieve better performance than with a lower frequency reuse factors; note, though, that this is true when there is no constraint in terms of BS density.

By looking at the single slope PL curve in Fig. 3, it appears that higher frequency reuse factors should still be preferred in order to improve the ASE vs coverage trade-off. However, unlike with the LOS/NLOS path loss, increasing the BS density enhances the ASE with no loss in terms of network coverage. Yet, modelling the signal propagation with the combined LOS/NLOS path loss yields different results than with the single-slope PL.

C. Partially loaded networks

In this subsection we show the results of the cell densification for partially loaded networks with LOS/NLOS propagation. Differently from the case of fully loaded networks, we recall that a fraction of the BSs may be inactive and, thus, the density of interfering BSs λ_I does not necessary follow the trend of BS density λ (see Section III-E and Fig. 1). In Fig. 4a and 4b we show the outage probability and the ASE curves, respectively, as function of the base station density for difference user densities. To better understand the effect of the partial load on the network performance, we compare these curves with those for fully loaded networks. We reported the values of the probability p_A of a BS being active over the outage and ASE curves.

We observe that, as long as $p_A \geq 0.9$, the deviation from the fully loaded network case is

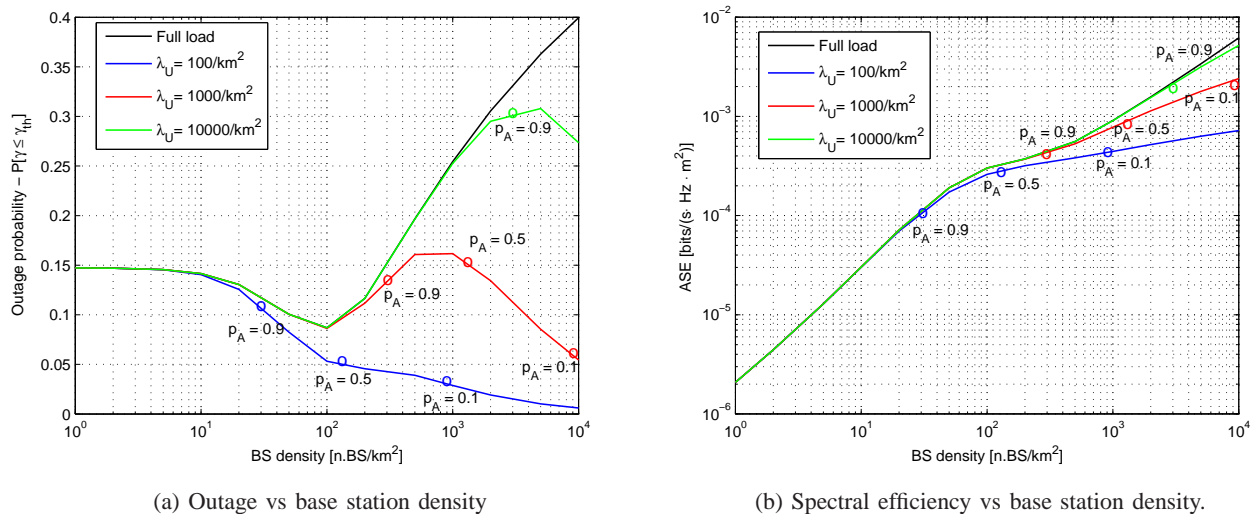


Fig. 4. The probability p_A given by (14) is reported as a dot on each curve. The outage probability has been obtained for $\gamma_{th} = -8\text{dB}$.

minimal. However, as soon as λ approaches the value of user density λ_U , the probability p_A drops and, as a consequence, the density of interfering λ_I BSs grows slowly with λ , up to the point where it saturates and converges to λ_U (see Fig. 1). At the same time, as λ increases, the distance from UE to the serving BS tends to decrease, leading to an increment of the received power. Overall, the fact that λ_I saturates whereas the received power keeps growing as λ increases has a positive impact on the SIR; as a result, the outage probability (see Fig. 4a) and the spectral efficiency improve once the density λ approaches or overcomes λ_U .

In regards to the ASE trend, we show the results in Fig. 4b. According to (20), the ASE trend is the combined outcome of the increase of the spectral efficiency and of the density of the active base stations. As the density of base stations increases and approaches the user density λ_U , the density of active base stations will converge to λ_U (see Fig. 4a); given that the density of active BSs remains constant, the only contribution to the ASE increase will be given by the spectral efficiency improvement. As a matter of fact, we can see that, with respect to the case of fully loaded networks, the ASE curves show a lower gain when the density λ approaches λ_U .

To assess steepness of the ASE, we applied linear regression to the ASE curves in order to obtain the value of the parameter α corresponding to different intervals of λ ; we specifically consider the approximation for the curve corresponding to $\lambda_U = 1000\text{UEs/km}^2$ (red curve in Fig. 4b). These values are $\alpha = 1.15$ within the density range 1-50 BSs/km², $\alpha = 0.43$ within

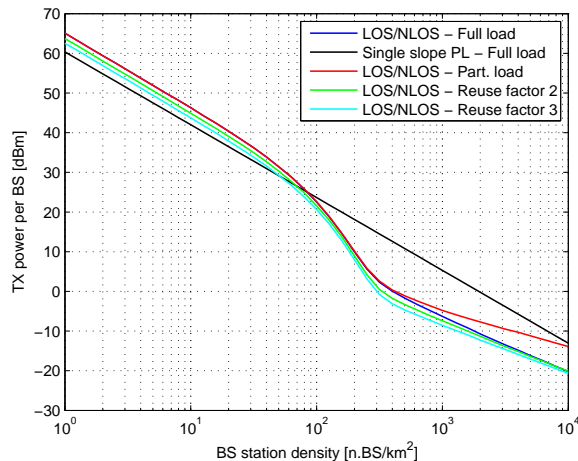


Fig. 5. Transmit power per BS. The power has been obtained with an SINR threshold $\gamma_{\text{th}} = -8\text{dB}$ and for tolerance $\Delta_{\theta} = 0.1\%$. The plot compares the TX power per BS for single slope-slope and LOS/NLOS path-loss for fully loaded networks. It also provides the curve for frequency reuse factor 2 and 3 and for partially loaded network with $\lambda_U = 1000\text{UEs/km}^2$.

the density range 50-500 BSs/km² and $\alpha = 0.46$ within the density range 500-10000 BSs/km².

D. Transmit power per base station

In Fig. 5 we show the simulation results of the transmit power per base station $P_{\text{TX}}(\lambda)$, which has been computed by using Algorithm 1 as explained in Section IV-A. In this figure we compare the results we obtained using the *single slope* and the *combined LOS/NLOS* path loss models.

As we can see from this plot, the behaviour of the transmit power as a function of the BS density λ is different in the two cases of single slope and combined LOS/NLOS propagation. With reference to Fig. 5, with single slope path loss, the power decreases linearly (in logarithmic scale) with the density; in the case of combined LOS/NLOS propagation, the transmit power exhibits different slopes as the as the base station density increases. We used linear regression to assess the slopes of the TX power curves (indicated by δ , as explained in Section IV-C) within different density intervals. With reference to the curve corresponding to fully loaded networks with LOS/NLOS propagation (solid-blue curve in Fig. 5), the values of (P_T, δ) are $(9.3 \cdot 10^{-9}, -1.9)$ within the λ range 1-60 BSs/km², $(4.4 \cdot 10^{-17}, -3.9)$ within the λ range 60-300 BSs/km² and $(1.15 \cdot 10^{-9}, -1.44)$ within the range 300-10000BSs/km².

The fact that the transmit power per base station decays more or less steeply with the density λ depends on how quickly the interference power increases or decreases with λ . As we explained

in Section IV-A, the transmit power per base station $P_{\text{TX}}(\lambda)$ has to be set so that the network is interference limited. Thus, if the channel attenuation between the interferer and the user decreases quickly as the density increases, a lower transmit power will be enough to guarantee that the interference power is greater than the noise power. In other words, if the interferer-to-user channel attenuation tends to decrease quickly as the density increases, so does the transmit power and vice-versa. For instance, for $\lambda \in [60, 300]$ BSs/km², the probability of having interferers in LOS with the user rises and, as a consequence, we have a lower attenuation of the channel between the interfering base station and the user. Hence, the $P_{\text{TX}}(\lambda)$ which guarantees the interference-limited regime will also decrease steeply with $\delta = -3.9$ as λ increases. On the contrary, for $\lambda > 300$ BSs/km², most of the interferers will have already entered the LOS zone, meaning that the interferer-to-user channel attenuation drops less rapidly than for $\lambda < 300$ BSs/km²; for this reason, also $P_{\text{TX}}(\lambda)$ will decrease less rapidly with $\delta = -1.44$.

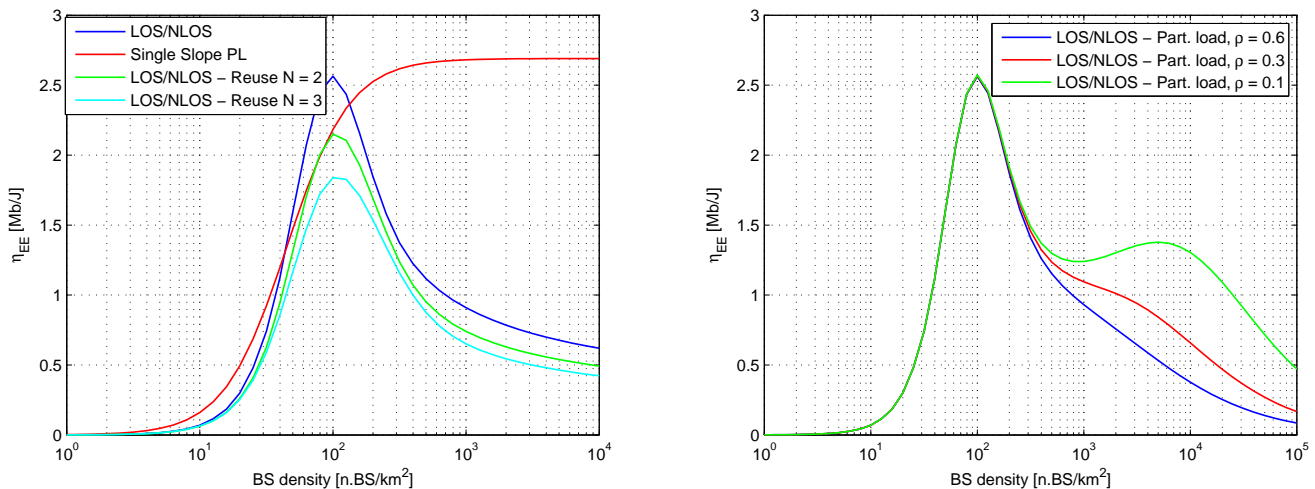
Let us note that, with increasing reuse factors N , the TX power decreases, as indeed a smaller bandwidth is used and, thus, the noise power is lower.

E. Energy efficiency

One of the most surprising outcomes of our study on LOS/NLOS propagation for ultra-dense networks is the effect of cell-densification on the energy efficiency of the fully loaded network, of which we show the results in Fig. 6a. The difference between the energy efficiency with single-slope and with LOS/NLOS path-loss is noticeable. In the case of single-slope PL, due to the linear growth of the ASE, $\eta_{\text{EE}}(\lambda)$ is a monotonically increasing function of the density λ (see Section IV-C1). In the case of LOS/NLOS propagation, from Fig. 6a we observe that the energy efficiency exhibits a maximum, which is achieved for a given density λ_0 .

To explain this, we consider the case frequency reuse $N = 1$ (solid-blue curve in Fig. 6a); from (29) and with the values of the parameters P_0 (given in Table I), P_{T} and δ (given in Section V-D), and α (given in Section V-A), the optimal point λ_0 is approximately 100BSs/km². Beyond this point, the ASE gain is too low to compensate power consumption increase in the network, leading to a drop in terms of energy efficiency. From Fig. 6a, we can note that frequency reuse reduces the energy efficiency compared to $N = 1$. As a result of the lower ASE achieved at higher frequency reuse factors N , the energy efficiency drops as N increases.

In Fig. 6b we show the energy efficiency for partially loaded networks, for a user density λ_{U}



(a) Energy efficiency for fully loaded networks.

(b) Energy efficiency for partially loaded networks.

Fig. 6. (a) Energy efficiency vs BS density for fully loaded networks. The plot compares the energy efficiency for LOS/NLOS with single slope path-loss. The energy efficiency is given also for frequency reuse factors 2 and 3. (b) Energy efficiency vs BS density for partially loaded networks. Curves are given for $\lambda_U = 1000$ UEs/km² and for three values of ρ .

of 1000 UEs/km². As we are dealing with partially loaded networks, we are interested in the BS densities $\lambda > \lambda_U$, where energy efficiency strongly depends on the power saving factor ρ of the BSs in stand-by state. This is because the parameter ρ determines the energy saving of the inactive BSs, which become more numerous as the density λ increases. Depending on the value of ρ , according to (33) a local maximum may even occur at $\lambda^* = \frac{\alpha\lambda_U(1-\rho)}{\rho(1-\alpha)}$.

With $\rho = 0.1$ and with the values of α given in Section V-C, the local maximum turns to be $\lambda^* \cong 7300$ BSs/km². For higher values of ρ , λ^* is smaller than or too close to λ_U to be considered as a reliable estimate of a maximum; we recall from Section IV-D that this estimate can be reckoned as reliable only if λ^* is sufficiently greater than λ_U . In fact, we observe from Fig. 6b that there is no local maximum beyond λ_U for $\rho = 0.3$ or 0.6.

VI. CONCLUSIONS

In this paper, we have proposed a stochastic geometry-based framework to model the outage probability, the Area Spectral Efficiency (ASE) of fully loaded and partially loaded Ultra-Dense Networks (UDNs), where the signal propagation accounts for LOS and NLOS components. We also studied the energy efficiency of UDNs resulting from this propagation model.

As the main findings of our work, we have shown that, with LOS/NLOS propagation, massive cell densification determines a deterioration of the network coverage at high cell densities, if the

network is fully loaded. Moreover, the ASE grows less steeply than a linear function at high cell densities, which implies that a larger number of base stations would be required to achieve a given throughput target with respect to the case of single slope path-loss. In regards to the energy efficiency, cell densification turns out to be inefficient for the network from an energetic point of view. In partially loaded networks, when the base station density exceeds that of the users, cell densification results in a coverage improvement. Overall, based on our findings, we can conclude that UDNs are likely face coverage issues in highly crowded environments with many users, which represent the worst case scenario for ultra-dense networks.

APPENDIX A

PDF OF THE DISTANCE TO THE SERVING BS

Once the LOS probability function is known, from (11) we obtain the PDF of the distance to the closest BS as follows:

$$P[r > R] = \exp\left(-\lambda \int_{B(0,R)} p_L(\|x\|) dx\right) \exp\left(-\lambda \int_{B(0,d_{\text{eq}}^{-1}(R))} (1 - p_L(\|x\|)) dx\right). \quad (\text{A.1})$$

Assuming the integrals in (A.1) can be solved in a closed-form, with some symbolic manipulation, (A.1) solves in its general form as follows:

$$P[r > R] = \prod_{m=1}^M \exp(f_m(R)). \quad (\text{A.2})$$

By taking the derivative of (A.2), we obtain:

$$\begin{aligned} \frac{d}{dR} [P[r > R]] &= \frac{d}{dR} \left[\prod_{m=1}^M \exp(f_m(R)) \right] = \sum_{m=1}^M \frac{d}{dR} [\exp(f_m(R))] \prod_{n=1, n \neq m}^M \exp(f_n(R)) = \\ &= \sum_{m=1}^M \frac{d}{dR} [f_m(R)] \exp(f_m(R)) \prod_{n=1, n \neq m}^M \exp(f_n(R)) = \sum_{m=1}^M f'_m(R) \prod_{n=1}^M \exp(f_n(R)) = \\ &= \sum_{m=1}^M f'_m(R) \left(\prod_{n=1}^M \exp(f_n(R)) \right) = P[r > R] \sum_{m=1}^M f'_m(R). \end{aligned} \quad (\text{A.3})$$

The PDF of the distance to the serving BS can finally be obtained as

$$f_r(R) = -\frac{d}{dR} [P[r > R]] = -P[r > R] \sum_{m=1}^M f'_m(R). \quad (\text{A.4})$$

If we assume the LOS probability to be given by (3), we can further develop (A.1) by solving the integrals in (A.1) and, with further symbolic manipulation, we obtain:

$$P[r > R] = e^{\pi\lambda L^2 e^{-\frac{R^2}{L^2}}} \cdot e^{-\pi\lambda L^2 e^{-\frac{R_{\text{eq}}^2}{L^2}}} \cdot e^{-\pi\lambda R_{\text{eq}}^2}, \quad (\text{A.5})$$

where $R_{\text{eq}} = d_{\text{eq}}^{-1}(R)$. Let us define the functions $f_1(R)$, $f_2(R)$, $f_3(R)$ and their first derivatives $f'_1(R)$, $f'_2(R)$, and $f'_3(R)$, respectively, as follows:

$$f_1(R) = \pi\lambda L^2 e^{-\frac{R^2}{L^2}}, \quad f_2(R) = -\pi\lambda L^2 e^{-\frac{R_{\text{eq}}^2}{L^2}}, \quad f_3(R) = -\pi\lambda R_{\text{eq}}^2, \quad f'_1(R) = -2\pi\lambda R e^{-\frac{R^2}{L^2}},$$

$$f'_2(R) = \pi\lambda K_{\text{eq}}^2 2\beta_{\text{eq}} R^{2\beta_{\text{eq}}-1} e^{-\frac{K_{\text{eq}}^2 R^{2\beta_{\text{eq}}}}{L^2}}, \quad f'_3(R) = -\pi\lambda K_{\text{eq}}^2 2\beta_{\text{eq}} R^{2\beta_{\text{eq}}-1}.$$

By plugging (A.5) and $f'_1(R)$, $f'_2(R)$, and $f'_3(R)$ in (A.4), we obtain the PDF of the distance to the serving BS.

When the LOS probability function is given by (4), we obtain the PDF of distance to the closest BS station as follows. First, by solving the integrals in (A.1) and by some additional algebraic operations, we obtain $P[r > R]$ as follows:

$$P[r > R] = e^{2\pi\lambda L^2 e^{-\frac{R}{L}}} \cdot e^{2\pi\lambda L R e^{-\frac{R}{L}}} \cdot e^{-\pi\lambda R_{\text{eq}}^2} \cdot e^{-2\pi\lambda L^2 e^{-\frac{R_{\text{eq}}}{L}}} \cdot e^{-2\pi\lambda L R_{\text{eq}} e^{-\frac{R_{\text{eq}}}{L}}}. \quad (\text{A.6})$$

Then, we define the functions $f_1(R)$, $f_2(R) \cdots$, $f_5(R)$ and we compute their respective derivatives $f'_1(R)$, $f'_2(R) \cdots$, $f'_5(R)$ as follows:

$$f_1(R) = 2\pi\lambda L^2 e^{-\frac{R}{L}}, \quad f'_1(R) = -2\pi\lambda L e^{-\frac{R}{L}}, \quad f_2(R) = 2\pi\lambda L R e^{-\frac{R}{L}}, \quad f'_2(R) = -2\pi\lambda(L-R)e^{-\frac{R}{L}},$$

$$f_3(R) = -\pi\lambda R_{\text{eq}}^2, \quad f'_3(R) = -\pi\lambda K_{\text{eq}}^2 2\beta_{\text{eq}} R^{2\beta_{\text{eq}}-1}, \quad f_4(R) = -2\pi\lambda L^2 e^{-\frac{R_{\text{eq}}}{L}},$$

$$f'_4(R) = 2\pi\lambda L K_{\text{eq}} \beta_{\text{eq}} R^{\beta_{\text{eq}}} e^{-\frac{K_{\text{eq}} R^{\beta_{\text{eq}}}}{L}}, \quad f_5(R) = -2\pi\lambda L R_{\text{eq}} e^{-\frac{R_{\text{eq}}}{L}},$$

$$f'_5(R) = 2\pi\lambda L K_{\text{eq}} \beta_{\text{eq}} R^{\beta_{\text{eq}}-1} (K_{\text{eq}} R^{\beta_{\text{eq}}} - L) e^{-\frac{K_{\text{eq}} R^{\beta_{\text{eq}}}}{L}},$$

Finally, the PDF can be obtained by plugging $f'_1(R)$, $f'_2(R) \cdots$, $f'_5(R)$ and (A.6) in (A.4).

REFERENCES

- [1] I. Hwang, B. Song, and S. S. Soliman, "A holistic view on hyper-dense heterogeneous and small cell networks," *IEEE Communications Magazine*, vol. 51, no. 6, pp. 20–27, Jun. 2013.
- [2] N. Bhushan, L. Junyi, D. Malladi, R. Gilmore, D. Brenner, A. Damnjanovic, R. Sukhvasi, and S. Geirhofer, "Network Densification: the Dominant Theme for Wireless Evolution into 5G," *IEEE Communications Magazine*, 2014.
- [3] J. Park, S.-L. Kim, and J. Zander, "Asymptotic behavior of ultra-dense cellular networks and its economic impact," in *IEEE Global Communications Conference (GLOBECOM 2014)*, Dec. 2014, pp. 4941–4946.
- [4] Ericsson, "Ericsson White paper: 5G radio access," Feb. 2015. [Online]. Available: www.ericsson.com/res/docs/whitepapers/wp-5g.pdf
- [5] J. G. Andrews, F. Baccelli, and R. K. Ganti, "A Tractable Approach to Coverage and Rate in Cellular Networks," *IEEE Trans. Wireless Commun.*, vol. 59, no. 11, pp. 3122–3134, 2011.

- [6] X. Zhang and J. G. Andrews, "Downlink Cellular Network Analysis with Multi-slope Path Loss Models," 2014. [Online]. Available: <http://arxiv.org/abs/1408.0549>
- [7] T. Bai, R. Vaze, and R. W. Heath, "Analysis of Blockage Effects on Urban Cellular Networks," *IEEE Trans. Wireless Commun.*, vol. 13, no. 9, pp. 5070–5083, Sep. 2014.
- [8] C. Galiotto, N. K. Pratas, N. Marchetti, and L. Doyle, "A Stochastic Geometry Framework for LOS/NLOS Propagation in Dense Small Cell Networks," *IEEE ICC 2015*, 2015. [Online]. Available: <http://arxiv.org/abs/1412.5065v2>
- [9] M. Ding, P. Wang, D. Lopez-Perez, G. Mao, and Z. Lin, "Performance Impact of LoS and NLoS Transmissions in Small Cell Networks," Mar. 2015. [Online]. Available: <http://arxiv.org/abs/1503.04251>
- [10] C. Li, J. Zhang, and K. B. Letaief, "Throughput and Energy Efficiency Analysis of Small Cell Networks with Multi-Antenna Base Stations," *IEEE Transactions on Wireless Communications*, vol. 13, no. 5, pp. 2505 – 2517, Mar. 2014.
- [11] T. Bai and R. W. Heath, "Coverage and Rate Analysis for Millimeter-Wave Cellular Networks," *IEEE Trans. Wireless Commun.*, vol. 14, no. 2, pp. 1536–1276, Oct. 2014.
- [12] S. Lee and K. Huang, "Coverage and Economy of Cellular Networks with Many Base Stations," *IEEE Commun. Lett.*, vol. 16, no. 7, pp. 1038–1040, Jul 2012.
- [13] H. S. Dhillon, R. K. Ganti, and J. G. Andrews, "Load-Aware Modeling and Analysis of Heterogeneous Cellular Networks," *IEEE Transactions on Wireless Communications*, vol. 12, no. 4, pp. 1666–1677, Apr. 2013.
- [14] 3rd Generation Partnership Project (3GPP), "Further Advancements for E-UTRA Physical Layer Aspects (Release 9)," Mar. 2010, 3GPP TR 36.814 V9.0.0 (2010-03).
- [15] B. Błaszczyszyn, M. K. Karray, and P. Keelerz, "Wireless networks appear Poissonian due to strong shadowing," *IEEE Transactions on Wireless Communications*, vol. PP, no. 99, pp. 1–1, 2015.
- [16] M. Haenggi, *Stochastic Geometry for Wireless Networks*. Cambridge Press, 2013.
- [17] F. Baccelli and B. Błaszczyszyn, *Stochastic Geometry and Wireless Networks, Volume I, Theory*. NOW Publishers, 2009.
- [18] V. Chandrasekhar and J. G. Andrews, "Spectrum Allocation in Tiered Cellular Networks," *IEEE Transaction on Communications*, vol. 57, no. 10, pp. 3059 – 3068, October 2009.
- [19] G. Auer *et al.*, "How Much Energy Is Needed to Run a Wireless Network?" *IEEE Wireless Commun.*, vol. 18, pp. 40 – 49, Oct. 2011.
- [20] I. Ashraf, F. Boccardi, and L. Ho, "SLEEP mode techniques for small cell deployments," *IEEE Communications Magazine*, vol. 49, no. 8, pp. 72–79, Aug. 2011.
- [21] C. Galiotto, I. M. Gomez, N. Marchetti, and L. Doyle, "Effect of LOS/NLOS Propagation on Area Spectral Efficiency and Energy Efficiency of Small-Cells," *IEEE Globecom 2014*, 2014. [Online]. Available: <http://arxiv.org/abs/1409.7575>